Published in Environ.Sci.&Techn. 53 (2019) 3823-3831

Dissolution and phosphate-induced transformation of ZnO nanoparticles in synthetic saliva probed by AGNES without previous solid-liquid separation. Comparison with UF-ICP-MS

Calin A. David, Josep Galceran, Federico Quattrini, Jaume Puy, Carlos Rey-Castro*

Departament de Química. Universitat de Lleida, and AGROTECNIO, Rovira Roure 191, 25198 Lleida (Spain)

* Corresponding author: *carlos.rey@quimica.udl.cat*

Abstract

The variation over time of free Zn^{2+} ion concentration in stirred dispersions of ZnO nanoparticles (ZnO NPs) prepared in synthetic saliva at pH 6.80 and 37º C was followed *in situ* (without solid-liquid separation step) with the electroanalytical technique AGNES (*Absence of Gradients and Nernstian Equilibrium Stripping*). At these conditions, ZnO NPs are chemically unstable due to their reaction with phosphates. The initial stage of transformation (around 5-10 h) involves the formation of a metastable solid (presumably $ZnHPO_4$), which later evolves into the more stable hopeite phase. The overall decay rate of ZnO NPs is significantly reduced in comparison with phosphate-free background solutions of the same ionic strength and pH. The effective equilibrium solubilities of ZnO (0.29 - 0.47 $mg \cdot L^{-1}$), as well as conditional excess-ligand stability constants and fractional distributions of soluble Zn species were determined in absence and presence of organic components. The results were compared with the conventional ultrafiltration and inductively coupled plasma-mass spectrometry (UF-ICP-MS) methodology. AGNES proves to be advantageous in terms of speed, reproducibility and access to speciation information.

Keywords: solubility, zinc oxide, ultrafiltration, oral exposure, bioavailability

Published in Environ.Sci.&Techn. 53 (2019) 3823-3831

1. Introduction

Zinc oxide nanoparticles (ZnO NPs) are increasingly used in rubber, ceramics, paints and personal care products such as skin creams and sunscreens.[1-3] The use of ZnO nanomaterials in dentistry has also attracted attention recently, due to their antimicrobial properties.[4,5] Some of the most common uses of ZnO NPs are generally regarded as safe for dermal application.[6,7] However, there are a number of studies reporting toxicological effects of ZnO NPs that might be relevant for other routes of exposure.[8] Quite often the key role of zinc ions released from NPs in the respective toxicity mechanisms is acknowledged.[9,10] Thus, some concerns are currently being raised about the safety of these materials with regards to oral exposure, due to their potential application in toothpastes, foods and food packaging.[11,12] As point of entrance to the gastrointestinal tract, the oral cavity represents a compartment of major interest for studies of risk assessment of ZnO NPs. Consequently, the knowledge of the fate and behaviour of these materials in saliva is very relevant. Despite that, and to the best of the authors' knowledge, no studies on the dissolution behaviour of ZnO in this biological fluid have been reported so far.

The investigation of the dissolution of nanomaterials is often complicated by the necessity of a solid-liquid separation step before elemental analysis. Different separation techniques have been proposed in the literature for this purpose.[13-15] One of the most common methods is ultrafiltration (UF), which involves the use of semipermeable filters (typically having pore sizes of 3 kDa) in a centrifugation tube. The filtrate collected after centrifugation is analysed subsequently by a suitable technique such as inductively coupled plasma-mass spectrometry (ICP-MS).[15,16] Even though UF is an affordable and robust technique, the use of an additional separation step in the analysis procedure adds a potential source of contamination and/or loss of

analyte, and increases the time required for sample pre-treatment, which can be particularly important if the rate of dissolution is to be tested.

On the other hand, the technique *Absence of Gradients and Nernstian Equilibrium Stripping* (AGNES)[17,18] has been proposed in recent years as an alternative method for the study of nanomaterial dissolution. AGNES measures directly free metal ion concentrations in aqueous (or hydro-alcoholic) solutions or dispersions. The determinands are amalgam-forming metallic elements such Cd, Pb or In,[19] but Zn has been the most extensively analysed so far.[20-28] AGNES has been applied, *e.g.*, to quantify adsorption of Pb or Cd onto latex[29-31] and TiO_2 nanoparticles,[32,33] to study the dissolution kinetics and equilibrium solubility of ZnO NPs,[34,35] to follow the dissolution of CdTe/CsS quantum dots,[36] to elucidate the role of ZnO NP dissolution in toxicity tests *in vitro* [37] and *in vivo,*[38] *etc*. One specific feature of AGNES is that it measures a well-defined chemical species (the free hydrated metal cation), in contrast to other operationally defined techniques (such as UF coupled to elemental analysis) that usually account for more than one chemical species (free ions plus soluble complexes of different molecular weights). Even though the total solubility (sum of all dissolved species of a given element) may be larger than the free ion concentration, especially in complex mixtures, AGNES still allows the estimation of solubility (in ligand-excess conditions) *via* a suitable titration procedure.[37] An important advantage of AGNES is that it can be applied directly to the dispersion without the need of any previous solid/liquid separation step.[14,15] In this way, it allows a good control over the environmental variables (pH, temperature) as well as a relatively short time of analysis, which is essential for the measurement of dissolution rates. However, up to date, no direct experimental comparison between AGNES and other separation/analysis coupled protocols has been reported. Thus, the aim of this work is to elucidate the dissolution behaviour of ZnO NPs dispersed in a surrogate medium for human saliva using AGNES

and to compare the results with the conventional UF-ICP-MS approach. A particular emphasis will be devoted to the role of phosphate and organic components of saliva on the dissolution rate of ZnO, the chemical speciation of the dissolved phase and the solid transformation species that may appear.

2. Materials and Methods

2.1 Materials

ZnO nanoparticles (material code JRCNM01100a, also known as NM110) were procured from the repository of the Joint Research Centre of the European Commission (Ispra, Italy), as one of the FP-7 NANoREG panel of representative nanomaterials. A summary of the physicochemical characterization data is included in the Supporting Information (SI).

Dissolved Zn solutions were prepared from a 1000 $mg \cdot L^{-1}$ standard solution (Certipur® Single-element ICP standard from Merck KGaA, Darmstadt, Germany). The composition of the synthetic saliva solutions is based on a recent *in vitro* human gastrointestinal model,[39] according to the recipe listed in Table **1**: saliva I (containing only the inorganic components) and saliva II (with both organic and inorganic components). All reagents within the synthetic saliva were purchased from Sigma-Aldrich Inc. (St. Louis, MO, USA) except mucin (from Carl Roth Gmbh & Co. KG, Karlsruhe, Germany).

2.2 Nanomaterial dispersion protocol

The NP dispersions were prepared by dilution from a 2.56 $mg \cdot mL^{-1}$ stock, which was obtained following the Standard Dispersion Protocol for ecotoxicological studies from NANoREG.[40] In brief, 25.6 mg of ZnO NPs were dispersed in 10 mL of Milli-Q water and sonicated at 5% amplitude (9.64±0.48 W), for 16 min with a Branson 250S sonicator (Thermo Fischer Scientific Inc., Waltham, MA, USA) using a 13 mm tip. The effectively delivered acoustic power of the probe sonicator was previously calibrated

following a calorimetric method, and the de-agglomeration performance was validated with appropriate benchmark materials.[40] The hydrodynamic sizes measured by Dynamic Light Scattering (DLS) are reported in the SI.

2.3 Dissolution Assays

The dissolution experiments were carried out by adding a suitable aliquot of the NP stock solution to a voltammetric thermostated cell containing the synthetic saliva. Previously, the background solutions were equilibrated at 37.0±0.1ºC and the desired pH (6.80±0.10) under a controlled atmosphere of 84±1 % N_2 (99.9990% purity) and 16±1 % CO_2 (99.995% purity) to remove traces of dissolved O_2, as it may interfere with voltammetric measurements. The gas mixture composition was controlled using two calibrated glass-tube variable area flowmeters (A6100 Series from ABB Ltd., Workington, UK) and it was checked with a nondispersive infrared carbon dioxide sensor (K33 ICB 30% CO_2 sensor from CO2Meter, Inc., Ormond Beach, FL, USA).

ZnO solubility is extremely sensitive to temperature and pH. In fact, a pH shift of half unit leads to a variation of up to 1 order of magnitude in the solubility.[34] For this reason, the dispersions were continuously monitored with a glass electrode attached to an Orion™ 720A+ pH-meter (from Thermo Fischer Scientific Inc., Waltham, MA, USA). The constant CO_2 partial pressure in the sample cell provided an adequate acid-base buffering. This buffering method, which was previously used in our laboratory,[23,37,41] is more representative of the environmental conditions in the oral cavity than the additions of strong acid or base. Indeed, the latter method might alter the composition of the synthetic saliva solutions or even (in the case of base additions) induce the formation of a hydrated $Zn(OH)_2$ layer on the NP surface.[34] Note that any possible differences in redox potential between the anoxic conditions in the testing vessel and actual oral cavity conditions are assumed irrelevant for ZnO dissolution, given the absence of reducing agents in the saliva recipe.

Control tests were carried out with dissolved Zn standard solutions instead of ZnO NPs. Ancillary experiments were also performed in absence of CO_2 atmosphere to discard the possible precipitation of solid carbonates.

Once the equilibrated saliva solutions were spiked with the NP stock solutions, three alternative routes were followed (as described in the following sections): *i*) the concentration of free Zn^{2+} ions was monitored continuously by AGNES; *ii*) the NP/saliva dispersions were sub-sampled into 20 mL Wheaton liquid scintillation glass vials, which were tightly sealed and incubated separately at 37ºC for 24h, and then measured by UF-ICP-MS; or *iii*) 1 mL of NP/saliva dispersion was pipetted into a 10 mm optical quartz cuvette for DLS or UV spectrophotometry measurements.

2.4 Measurement of free Zn^{2+} concentrations

The concentration of free Zn^{2+} ions, $[Zn^{2+}]$, was measured directly in the saliva media by AGNES without any prior solid/liquid separation step. AGNES is a voltammetric technique entailing two stages: deposition and stripping, for which different procedures or variants can be used. In AGNES-I, the variant used here,[18] the stripping current (I) is measured at a fixed time after the application of an oxidation potential in the diffusion-limited regime. The current is proportional to the free metal concentration in the bulk sample. The proportionality constant is the product of a calibration factor (η) and a gain or pre-concentration factor (Y) that can be adjusted by selecting the applied deposition potential. The two-potential-pulse mode was used in the deposition stage.[42] Other operational parameters are summarized in the SI. These settings allowed a time lapse between consecutive measurements of *ca*. 5 min, which is fast enough to track the evolution of $[Zn^{2+}]$ during dissolution/transformation of ZnO (see Results section). The electrochemical measurements were carried out with an Autolab PGSTAT12 potentiostat and a 663VA stand (both from Metrohm AG, Herisau, Switzerland) using a multimode mercury drop electrode (drop radius of 1.41×10^{-4} m), an auxiliary glassy

carbon electrode, and an Ag/AgCl/3 mol·L^{-1} KCl reference electrode, also from Metrohm. During the application of AGNES, the N_2/CO_2 gas mixture flowed continuously through the headspace of the voltammetric cell.

2.5 Other Experimental Methods

The average hydrodynamic diameters and zeta-potential values were measured by Dynamic Light Scattering (DLS) using a Zetasizer Nano-ZS (Malvern instruments Ltd., Worcestershire, UK) with a He-Ne laser of 633 nm wavelength, at an angle of 173°. The autocorrelation functions were analysed with the standard method of cumulants to obtain the intensity-weighted particle size distributions. The viscosity of the dispersions was assumed equal to that of pure water at the same temperature, the refractive index of ZnO was taken as 2.004,[43,44] and the attenuation factor and laser position were set to automatic. Zeta potentials were measured by Laser Doppler Micro-electrophoresis using also the Zetasizer Nano-ZS. The electrophoretic mobility measurements were transformed using Henry's equation under Smoluchowski approximation.[45]

The characteristic absorption spectra of ZnO NPs in dispersion (with a maximum at λ=371 nm) was followed by time-resolved UV-vis spectrophotometry using a Lambda XLS spectrophotometer (from PerkinElmer, Inc., Waltham, MA, USA). This provided a direct measurement of the rate of transformation of ZnO in saliva.[34]

The solid-liquid fractionation of the dispersions by ultrafiltration (UF) was carried out with Amicon® Ultra-15 centrifugal filter units (from Merck KGaA, Darmstadt, Germany) containing a cellulose membrane of 3 kDa molecular weight cut-off.[13] In this procedure, 10 mL samples were ultra-filtered at a relative centrifugal field (RCF) of 5000g for 15 min. After UF, 2 mL were taken from each filtrate and acidified with HNO_3 for subsequent elemental analysis. Then, the total concentration of dissolved Zn, $c_{T,Zn}$, was measured by inductively coupled plasma (ICP-MS) using a 7700 Series instrument from Agilent Technologies, Inc. (Santa Clara, CA, USA).

3. Results and discussion

It has been shown that the equilibrium solubility of ZnO NPs increases as the size of primary particles becomes smaller due to the effect of interfacial tension, according to the Ostwald-Freundlich equation.[34] Due to its relatively large radius (*ca*. 74 nm), the NM110 material is expected to have practically the same solubility as bulk ZnO (see SI). Indeed, the theoretical value of $[Zn^{2+}]$ in equilibrium with bulk ZnO at 37ºC dispersed in a non-complexing solution at the same pH (6.8) and ionic strength (0.0586 $mol \cdot L^{-1}$) as saliva is 1.8×10^{-3} $mol \cdot L^{-1}$ (equivalent to 150 mg $ZnO \cdot L^{-1}$), whereas the Ostwald-Freundlich prediction for NM110 at the same conditions is 157 mg $ZnO \cdot L^{-1}$. Note that, in presence of Zn-complexing ligands (such as those present in saliva) the solubility of ZnO is even larger, as it comprises the sum of all dissolved species of Zn. However, speciation calculations with the program Visual MINTEQ[46] for the specific composition of saliva I (the organic components of saliva II are not included in the standard thermodynamic database) predict oversaturation of zinc phosphate or carbonate salts already at much lower Zn concentrations (as will be discussed later). Therefore, the first goal was to investigate the time variation of the free Zn^{2+} concentration in the dispersions after the addition of increasing amounts of ZnO NPs to either saliva I or saliva II. The comparison between both media allows us to estimate the chemical speciation of the dissolved phase and, in particular, the role of the organic components on the solubility. The following subsections summarize the observed behaviour of the dispersions regarding their aggregation and dissolution. In the latter case, we discuss separately the results obtained below and above saturation conditions.

3.1 Stability of ZnO dispersions

The initial hydrodynamic diameters of ZnO NPs measured by DLS in saliva at a total Zn concentration of 10^{-3} $mol \cdot L^{-1}$ (231.2±3.2 nm) were very similar to the stock solution (see SI) and remained constant during the first 3 hours of the experiments. The zeta

potential of ZnO particles in the saliva was -35.9±1 mV, whereas a value of 9.7±1.5 mV was measured in a KCl solution at the same ionic strength (and fast aggregation was observed within 30 minutes). These results suggest that phosphate is adsorbed on the surface of NPs at the initial stages,[47] which stabilizes the dispersions against aggregation through an electrostatic mechanism. This fact would be relevant for the chemical stability of the NPs, since small particle size distributions lead to large effective surface areas and, consequently, fast rates of transformation of the ZnO NPs either by dissolution[34] or by precipitation of inorganic coatings on the particles' surface. However, the DLS measurements are not reliable enough to track the corresponding changes in the average size.

3.2 Undersaturated solutions

Additions of ZnO NPs to saliva I and II below total Zn concentrations of 4-6×10^{-6} mol·L^{-1} (0.3-0.5 mg ZnO·L^{-1}) led to a fast and complete dissolution of the NPs. Consequently, the values of [Zn^{2+}] reached a constant value within a few minutes after each addition (below the time resolution of AGNES). This high rate of dissolution is consistent with a reaction-diffusion model reported previously,[34] given the small particle size distribution of the NPs.

The values of [Zn^{2+}] were proportional to the total Zn concentration, $[Zn]_{total}$, (Fig 1), as expected for a medium composition containing organic/inorganic ligands in excess with respect to the metal. Indeed, the mass balance of Zn prescribes:

$$\begin{aligned} c_{\mathrm{T,Zn}} &= \left[\mathrm{Zn^{2+}}\right] + \left[\mathrm{ZnHPO_{4,}}_{aq}\right] + \left[\mathrm{ZnHCO_3^+}\right] + \left[\mathrm{ZnSO_{4,}}_{aq}\right] + \left[\mathrm{ZnCO_{3,}}_{aq}\right] + \left[\mathrm{ZnL}\right] + \ldots = \\ &= \left[\mathrm{Zn^{2+}}\right]\left\{1 + K'_{\mathrm{ZnHPO_{4,}}_{aq}} + K'_{\mathrm{ZnHCO_3^+}} + K'_{\mathrm{ZnSO_{4,}}_{aq}} + K'_{\mathrm{ZnCO_{3,}}_{aq}} + K'_{\mathrm{ZnL}} + \ldots.\right\} = \\ &= \left[\mathrm{Zn^{2+}}\right]\left\{1 + K'_{\mathrm{inorg}} + K'_{\mathrm{org}}\right\} = \\ &= \left[\mathrm{Zn^{2+}}\right]\left\{1 + K'_{\mathrm{medium}}\right\} \end{aligned} \quad (1)$$

Where $c_{T,Zn}$ is the total concentration of dissolved Zn (equal to $[Zn]_{total}$ only in the case of complete dissolution such as this), and Zn^{2+}, $ZnHPO_{4,aq}$, $ZnHCO_3^+$, $ZnSO_{4,aq}$, $ZnCO_{3,aq}$ are the major inorganic dissolved species of Zn (according to Visual MINTEQ). L represents a generic organic ligand, and K'_j indicates the conditional stability constant for the formation of species *j* (*i.e.*, the stability constant times the concentration of free ligand). By definition, K'_j has a constant value under excess of ligand conditions. In eq. (1), K'_{medium} is the collective conditional stability constant of the dissolved complexes of Zn, which splits into K'_{inorg} and K'_{org}, the collective terms corresponding to the inorganic and organic complexes. Eq. (1) allows AGNES to estimate the total solubility of ZnO in saturated dispersions, as will be discussed later. Let us rearrange eq. (1) into a log scale:

$$\log\left[Zn^{2+}\right] = \log c_{T,Zn} - \log\left\{1 + K'_{medium}\right\} \quad (2)$$

This linear relationship was confirmed by AGNES measurements in both saliva I and II (see Fig 1). As expected, the value of K'_{medium} calculated from experimental data using eq. (2) depends on the composition of the medium. In the case of saliva I, which has only inorganic components, the value of the collective stability constant was estimated as $K'_{saliva\ I} = K'_{inorg} = 2.2 \pm 0.1$, in agreement with the theoretical value from Visual MINTEQ, $K'_{inorg,theor.} = 1.95$. In the case of saliva II, with both organic and inorganic complexes, the absolute value of the intercept in eq. (2) is larger (*i.e.*, the plot is shifted towards lower free Zn^{2+} concentrations). This leads to a value of $K'_{saliva\ II} = K'_{inorg} + K'_{org} = 4.1 \pm 0.3$, which, in turn, yields $K'_{org} = 1.9 \pm 0.3$. The latter value could not be compared with Visual MINTEQ because of the lack of stability constants in the database for complexes of Zn with ligands such as amylase or urea (although a

value of $K'_{\text{Zn-urea}} \approx 0.58$ was estimated from dedicated AGNES experiments, see SI). These results indicate a larger complexation capacity of saliva II (due to the contribution of organic ligands) leading to lower free concentrations compared with saliva I at the same total Zn concentrations.

The theoretical distribution of Zn species in the dissolved phase is calculated straightforwardly from the values of K'_j, leading to the following results: approximately 20% of dissolved Zn corresponds to free Zn^{2+} ions, 43% to inorganic complexes and 37% to organic complexes (11% Zn-urea plus 26% of high molecular weight complexes like amylase and mucin). Note that this distribution is independent of the total (dissolved plus particulated) Zn concentration, and it is also expected to hold in saturated solutions at equilibrium, as long as excess of ligand conditions are fulfilled.

3.3 Saturated solutions

3.3.1 Time evolution of $[Zn^{2+}]$

Large additions of ZnO NP stock solution to saliva (above 0.5 mg $ZnO \cdot L^{-1}$) led to a complex dynamic response of AGNES measurements. The evolution of $[Zn^{2+}]$ with time showed an initial plateau around $[Zn^{2+}]=10^{-5}$ $mol \cdot L^{-1}$ (Fig 2) and remained constant (or decreased very slowly) over a period of 300 to 600 minutes after the NP spike. Then, it suddenly dropped down to *ca*. $[Zn^{2+}]=10^{-6}$ $mol \cdot L^{-1}$, and this final value was quite sensitive to small fluctuations in pH. The length of the initial plateau had a low reproducibility, without clear correlations with NP concentration, stirring rate, exact pH, etc. On the contrary, the final stable (equilibrium) value of $[Zn^{2+}]$ was very reproducible and clearly related with the exact pH of the dispersion. This equilibrium value was also consistent with the solubility of hopeite ($Zn_3(PO_4)_2 \cdot 4H_2O$), as supported by Visual MINTEQ and discussed in next section. The hypothesis of hopeite as the final solid phase is supported by several studies on the reactivity of ZnO with phosphate,[47-51]

277 which report a high sensitivity of the composition and structure of the solid on the
278 environmental variables like pH.[47]
279 Noteworthy, the existence of a metastable regime occurs both in saliva I and II (Fig 2),
280 and its duration does not seem related with the presence of organic components. This
281 discards the possibility that the growth of an organic coating on the NP surface caused
282 the initial quasi-steady state in the [Zn^{2+}] *vs*. time plots.
283 The evolution of the concentration of solid ZnO with time was also monitored by UV-
284 vis spectrophotometry in parallel to AGNES measurements (Fig SI-2). The data indicate
285 that the concentration of ZnO decays very slowly during the first few hours after the NP
286 addition until it suddenly drops down to zero. These long decay times are consistent
287 with the length of the plateaus observed in the simultaneous AGNES measurements of
288 [Zn^{2+}]. Moreover, the complete disappearance of the ZnO absorption band coincides
289 with the achievement of the equilibrium value of [Zn^{2+}] ruled by the solubility product
290 of hopeite. An ancillary experiment following the dissolution of ZnO NPs in a KCl
291 solution (in absence of phosphate) at the same temperature, pH and ionic strength
292 revealed that the half-life of ZnO in these conditions is around 12 min (see also Fig SI-
293 2), in agreement with previous kinetic studies.[34] These findings suggest that the
294 effective rate of dissolution of ZnO NPs in synthetic saliva is modulated by the presence
295 of phosphate, which increases the half time by a factor of 25-50. This conclusion is also
296 supported by the results of other authors,[48] who reported a substantial increase in the
297 dissolution times of ZnO NPs in presence of phosphate, compared with similar solutions
298 where phosphate was absent. Thus, it can be safely concluded that phosphate hinders
299 the kinetics of dissolution of ZnO NPs, even though the free Zn^{2+} concentration is
300 relatively low due to hopeite precipitation.
301 The initial plateau in the dynamic evolution of [Zn^{2+}] was also observed in the control
302 experiments where a dissolved Zn standard was added to the synthetic saliva instead of

303 ZnO NPs (see Fig SI-3 and one representative example in Fig 1). Indeed, the titration of
304 saliva with dissolved Zn also led to metastable regimes of variable duration between
305 300 and 500 minutes, while free ion concentrations remained around -log [Zn^{2+}]=5.0-
306 5.2 (well below the total Zn concentrations in all cases). During this period, a precipitate
307 was formed (the solution became slightly cloudy), but it was not possible to isolate it or
308 characterize it further. This metastable phase cannot be ascribed to Zn carbonate, since
309 it appears also in those titration experiments where all carbonate species were stripped
310 off the synthetic saliva by N_2 purging (Fig SI-3). Note also that, after the plateau, [Zn^{2+}]
311 values dropped down quickly to stable values around -log [Zn^{2+}]=5.8-6.0, once again in
312 agreement with the solubility of $Zn_3(PO_4)_2 \cdot 4H_2O$ as calculated by Visual MINTEQ.
313 Ancillary AGNES experiments consisting of Zn titrations of synthetic saliva solutions
314 without phosphates, but equilibrated with respect to the $CO_2/\ HCO_3^-$ system, did not
315 show indications of precipitation at comparable Zn concentrations (see SI).
316 Nevertheless, the possibility of co-precipitation of carbonates and phosphates of Zn in
317 the whole saliva cannot be completely ruled out.
318 The experimental information gathered is consistent with the following mechanism of
319 concurrent ZnO dissolution and zinc phosphate precipitation:

320
$$\begin{aligned} &ZnO_{(s)} + \text{saliva} \xrightarrow{fast} PO_4^{-3}\text{-coated } ZnO_{(s)} \xrightarrow{fast} \\ &\xrightarrow{fast} Zn^{+2} + HPO_4^{-2} \rightleftharpoons ZnHPO_{4(s)} \xrightarrow{slow} Zn_3(PO_4)_2 \cdot 4H_2O_{(s)} \end{aligned} \quad (3)$$

321 According to this mechanism, the Zn^{2+} ions released from ZnO NPs at the earliest
322 stages would quickly react with the phosphate species in solution to form different
323 soluble complexes as well as an intermediate solid, which could be ascribed to $ZnHPO_4$.
324 This intermediate phase, probably of amorphous nature, would precipitate faster than
325 hopeite despite being less stable.[49,51] At the same time, a complex chemical and
326 structural transformation of the ZnO NP surface might occur involving, *e.g.*
327 development of a $Zn(OH)_2$ coating, adsorption of phosphate anions (as suggested by the

zeta potential), OH^-/PO_4^{3-} exchange resulting in the formation of an amorphous zinc phosphate layer,[48] *etc*. The hypothetical formation of this surface coating on the ZnO NPs would result in a decreased overall rate of dissolution.[47] Accordingly, the value of $[Zn^{2+}]$ in solution would be effectively buffered by the precipitation of $ZnHPO_{4(s)}$, thus showing an apparent plateau in the dynamic behaviour. A pseudo-steady state would settle where the rate of Zn^{2+} release from ZnO dissolution becomes similar to the rate of transformation of $ZnHPO_{4(s)}$ into hopeite. When crystallization of hopeite (the rate-limiting step) is completed and all $ZnHPO_{4(s)}$ is exhausted, the value of $[Zn^{2+}]$ in solution would quickly drop down to the value in equilibrium with $Zn_3(PO_4)_2{\cdot}4H_2O_{(s)}$.

If this mechanism is correct, it would also explain the existence of a plateau during the titration experiments with dissolved Zn standards. In this case, the steady-state value of the free Zn^{2+} concentration would be $\left[Zn^{2+}\right] = K_{sp,ZnHPO_4} / \gamma_{\pm}^2 \left[HPO_4^{2-}\right]$, assuming conditions of equilibrium and excess of phosphate species, with $K_{sp,ZnHPO_4}$ being the solubility product of $ZnHPO_{4(s)}$ and $\gamma_{\pm}$ the mean ion activity coefficient. An estimate of $K_{sp,ZnHPO_4}$ at 37ºC was obtained from AGNES experiments, as detailed in the SI. Theoretical predictions of $[Zn^{2+}]$ in equilibrium with $ZnHPO_{4(s)}$ were calculated with Visual MINTEQ using this value of $K_{sp,ZnHPO_4}$. The results are represented as the upper dashed red line in Fig 1. Note that the line bends upwards slightly at large values of $[Zn]_{total}$ due to the depletion of ligands (this indicates the upper boundary of ligand excess conditions).

Finally, the assumption that the overall rate of transformation is limited by the hopeite crystallization step also explains why the behaviour of the $[Zn^{2+}]$ *vs.* time curves in the titrations with NPs and Zn standards are so similar.

3.3.2 $[Zn^{2+}]$ at equilibrium and effective solubility

As mentioned above, the final value of $[Zn^{2+}]$ (after a sufficiently large addition of Zn) is consistent with the solubility equilibrium of hopeite, the thermodynamically stable phase. Since there is sufficient excess of phosphates in solution, the law of mass action constrains $[Zn^{2+}]$ at equilibrium to a constant value that depends on pH, but not on the total Zn concentration:

$$\left[Zn^{2+}\right]_{eq} = \left(\frac{K_{sp,hopeite}}{\gamma_{\pm}^{5}\left[PO_4^{3-}\right]^2} \right)^{1/3} \quad (4)$$

A value of $[Zn^{2+}]_{eq}=1.15\times10^{-6}$ mol·L^{-1} ($-\log[Zn^{2+}]_{eq}=5.94$) at pH 6.80 was calculated using Visual MINTEQ with Davies correction of ion activity coefficients and a solubility product for hopeite at 37ºC of $-\log K_{sp,hopeite,37°C} = 35.74$.[52] It must be pointed out that the standard thermodynamic database of Visual MINTEQ contains only the value at 25ºC ($-\log K_{sp,hopeite,25°C} = 35.42$) and does not include an estimate of the enthalpy of dissolution. Interestingly, hopeite shows a retrograde solubility with temperature like zincite (ZnO).

Eq. 4 applies whenever the liquid phase is in equilibrium with hopeite, regardless the presence of any dissolved ligands in solution that might form complexes with Zn, which would only increase the overall solubility of hopeite, but not affect the value of $[Zn^{2+}]$. Therefore, this equation is valid for both saliva I and II.

Eq. 4 is represented as a continuous red line in Fig 1. Experimental AGNES results obtained in equilibrated dispersions of saliva I and II for $[Zn]_{total}>10^{-4}$ mol·L^{-1} are in excellent agreement with this prediction, with a value of $[Zn^{2+}]_{eq}=(1.13\pm0.08)\times10^{-6}$ mol·L^{-1}, or $-\log[Zn^{2+}]_{eq}=5.95\pm0.03$. As already mentioned, the titrations performed with Zn standard (instead of ZnO NPs) yielded similar results. It must be noted that for Zn additions in the low range of oversaturation conditions, *i.e.*: 10^{-5} mol·L$^{-1}<[Zn]_{total}<10^{-4}$

mol·L^{-1}, the metastable regime did not evolve towards the hopeite equilibrium within the timespan of the experiments (Fig 1), due to the relatively small value of the oversaturation index.

Finally, we define the *effective* (or *apparent*) solubility of ZnO NPs in saliva, *s*, as the maximum concentration of ZnO that can be dissolved right before the thermodynamic saturation of hopeite is achieved (which is, in fact, equivalent to the solubility of hopeite in the medium). This value can be calculated, for each saliva composition, from the intersection of eq. 2 (the value of $[Zn^{2+}]$ corresponding to full dissolution of ZnO) and eq. 4 (the value of $[Zn^{2+}]_{eq}$ in equilibrium with hopeite):

$$s = \left[Zn^{2+} \right]_{eq} \left\{ 1 + K'_{medium} \right\} \quad (5)$$

Where K'_{medium} depends on the sample composition. This procedure yielded s=(3.6±0.3)×10^{-6} mol·L^{-1} (0.29 mg ZnO·L^{-1}) and s=(5.7±0.8)×10^{-6} mol·L^{-1} (0.47 mg ZnO·L^{-1}) for saliva I and II, respectively. As expected from the contribution of the organic ligands, the solubility of ZnO NPs is larger in the latter case.

3.4 Comparison of UF-ICP-MS and AGNES

The results of the dissolution assays measured by UF-ICP-MS are shown in Fig. 3, where the total dissolved concentration of Zn in the filtrate ($c_{T,Zn}$) is plotted as a function of $[Zn]_{total}$. Two main sources of experimental uncertainty were identified. First, there was some loss of analyte in the undersaturated solutions due to adsorption of Zn species on the UF membranes. The effective recovery in UF was quantified, from filtration tests with Zn standards, as 70% (mean value) of the total dissolved Zn, without significant differences between saliva I and II. In the latter case, the loss of analyte might also be due to the complexation of Zn to large molecular weight organic ligands (which should be retained in the filters). The uncertainty of the experimental data, however, does not allow discriminating between both fractions (metal directly adsorbed

on the membrane and metal retained as large organic molecules). Second, and more importantly, the small volume of N_2/CO_2 mixture in the headspace of the sample vials was not enough to buffer pH properly during incubation, especially at the highest NP doses. Therefore, the final pH values measured after 24 h, right before centrifugation, were shifted to the alkaline region by 0.2-1.2 units due to the release of OH^- ions during the dissolution of ZnO. Therefore, the following approximate theoretical correction is proposed for those samples above the saturation point of hopeite:

$$\left(c_{\mathrm{T,Zn}}\right)^{\mathrm{pH}\,6.8}_{\text{UF-ICP-MS}} = \left(c_{\mathrm{T,Zn}}\right)^{\mathrm{pH\ exp}}_{\text{UF-ICP-MS}} \times \frac{s^{\mathrm{pH}\,6.8}}{s^{\mathrm{pH\ exp}}} \qquad (6)$$

Where $\mathrm{pH_{exp}}$ is the value measured in each vial after incubation, and $s^{\mathrm{pH}i}$ is the theoretical concentration of dissolved Zn species in equilibrium with hopeite in saliva at 37ºC and pH *i*, calculated with Visual MINTEQ. Since only the inorganic components are included in the standard thermodynamic database, a value of $K'_{\mathrm{Zn\ urea}} = 0.58$ was included in the calculations for saliva II as the conditional formation constant of Zn-urea complexes, which were the only organic Zn species theoretically able to pass through the 3kDa filters.

The corrected UF-ICP-MS results are plotted in Fig. 3 (lower panel) together with the effective solubilities in saliva I and II (blue and green horizontal lines, respectively) calculated from AGNES results using eq. (5). The theoretical correction reduces the experimental uncertainty and improves significantly the agreement between UF-ICP-MS and AGNES, especially in the absence of organic components (saliva I). In saliva II, however, the UF results overestimate the solubility value obtained with AGNES. This is particularly remarkable, given that UF should remove the organic complexes of large molecular weight, which represent a significant fraction of the dissolved Zn. This overestimation might be due to an excessive correction of the pH shifts or to further changes in environmental conditions during centrifugation. In any case, the modest

accuracy of the UF-ICP-MS data of saliva II does not enable an indirect estimation of the fraction of high molecular weight organic complexes of Zn.

4. Relevance for nanosafety assessment

There are currently no regulatory guidelines for bioavailability and zinc release from nanomaterials to serve as a comparison for this work, but some useful insights can be extracted nonetheless. The fact that small concentrations of NM110 dissolve completely in the timescale of a few minutes, suggests that oral exposure to ZnO NPs might be assimilated to the case of conventional (non-nano) soluble Zn species at low doses. Additionally, chemical speciation of the dissolved phase (20% of Zn in the form of free ions) points to a relatively large bioavailability to the oral cavity microbiota. At high ZnO concentrations, the dissolution is hindered by the formation of intermediate metastable solid phases, while the whole transformation into hopeite takes place within 5-8 hours under vigorous stirring. This slow kinetics indicates that metastable and partially phosphate-converted solid nanoparticles might be transported through the upper gastrointestinal tract after ingestion. Even though ZnO and its phosphate-transformation products are expected to completely dissolve in the low pH environment of the stomach,[11] the mucus and epithelial tissue of the oesophagus would still be exposed to them.[53] This supports the need for further risk assessment studies that take into account the aging processes of ingested ZnO particles during transit throughout the upper digestive tract.

The extrapolation of these results to the evaluation of fate after oral exposure in real conditions should be considered with caution. Firstly, the NM110 material chosen for this study, although a representative model material for the testing of regulatory-relevant endpoints,[1] is not specifically intended for oral intake. The general findings presented here should be further checked with ZnO nanomaterials designed for other

450 purposes and, in this way, correlations with physicochemical features such as particle
451 size, presence of synthetic organic coatings, etc. could be established. Secondly, recent
452 works with Ag NPs have reported that reactivity in natural human saliva samples might
453 be lower than in synthetic surrogate solutions.[54] However, in this respect, the
454 comparison between saliva I and II shows no indication that organic matter may
455 decrease the ZnO dissolution rate. Finally, the actual *in vivo* conditions prevailing in the
456 oral cavity certainly differ from those adopted in the present *in vitro* study, in terms of
457 fluctuations of pH and redox potential, presence of microbial flora and co-ingested
458 material, hydrodynamics and shear forces, etc.[11,12,55] Despite all these shortcomings, this
459 work represents a proof of concept demonstration of the advantages of electroanalytical
460 techniques like AGNES for the equilibrium speciation and dynamics of transformation
461 of nanomaterials in natural fluid solutions, as compared with fractionation/elemental
462 analysis coupled methods such as UF-ICP-MS. In this respect, AGNES may be valuable
463 as an analytical tool for regulatory testing procedures.

464 ## Associated content

465 **Supporting information (SI)**. Physicochemical characterization data of NM110 ZnO;
466 de-agglomeration performance of the probe sonicator; equilibrium solubility of ZnO
467 nanomaterials; settings used in AGNES experiments; simultaneous UV-vis
468 spectrophotometry and AGNES measurements; determination of Zn-urea conditional
469 binding constant; titrations of saliva I with dissolved Zn standard solutions; titration of
470 saliva I in absence of phosphates; determination of the solubility product of $ZnHPO_4$
471 (PDF).

472 ## Disclosure statement

473 The authors report no conflict of interest.

474 ## Acknowledgments

475 This work was supported by the Spanish Ministry MINECO under Grant CTM2016-
476 78798 and European Union Seventh Framework Programme FP7-NMP.2012.1.3-3
477 under Grant no. 310584 (NANoREG). FQ gratefully acknowledges a grant from
478 AGAUR. The authors thank Dr. A. Altier for her technical assistance with DLS
479 measurements.

480

References

(1) Singh, C.; Friedrichs, S.; Levin, M.; Birkedal, R.; Jensen, K.; Pojana, G.; Wohlleben, W.; Schulte, S.; Wiench, K.; Turney, T.; Koulaeva, O.; Marshall, D.; Hund-Rinke, K.; Kördel, W.; Doren, E. V.; Temmerman, P.-J. D.; Francisco, M. A. D.; Mast, J.; Gibson, N.; Koeber, R.; Linsinger, T.;Klein, C. L., *NM-series of representative manufactured nanomaterials: Zinc oxide NM-110, NM-111, NM-112, NM-113 characterisation and test item preparation*, Report EUR 25066 EN, Joint Research Centre – Institute for Reference Materials and Measurements, Luxembourg, 2011.

(2) Project on Emerging Nanotechnologies (2013). Consumer Products Inventory, http://www.nanotechproject.org/cpi.

(3) Lead, J. R.;Valsami-Jones, E., Eds. *Nanoscience and the Environment*, Elsevier: Amsterdam, The Netherlands, 2014.

(4) Abdulkareem, E. H.; Memarzadeh, K.; Allaker, R. P.; Huang, J.; Pratten, J.;Spratt, D. Anti-biofilm activity of zinc oxide and hydroxyapatite nanoparticles as dental implant coating materials. *J. Dent.* **2015**, *43* (12), 1462-1469.

(5) Esteban-Tejeda, L.; Cabal, B.; Torrecillas, R.; Prado, C.; Fernandez-Garcia, E.; Lopez-Piriz, R.; Quintero, F.; Pou, J.; Penide, J.;Moya, J. S. Antimicrobial activity of submicron glass fibres incorporated as a filler to a dental sealer. *Biomed. Mater.* **2016**, *11* (4), 045014.

(6) SCCS (Scientific Committee on Consumer Safety), *Opinion on ZnO (nano form) COLIPA S 76 (SCCS/1489/12)*, European Commission, 2012.

(7) SCCS (Scientific Committee on Consumer Safety), *ADDENDUM to the Opinion SCCS/1489/12 on Zinc oxide (nano form), 23 July 2013, revision of 22 April 2014*, European Commission, 2013.

(8) Liu, J.; Feng, X. L.; Wei, L. M.; Chen, L. J.; Song, B.;Shao, L. Q. The toxicology of ion-shedding zinc oxide nanoparticles. *Crit. Rev. Toxicol.* **2016**, *46* (4), 348-384.

(9) Golbamaki, N.; Rasulev, B.; Cassano, A.; Robinson, R. L. M.; Benfenati, E.; Leszczynski, J.;Cronin, M. T. D. Genotoxicity of metal oxide nanomaterials: review of recent data and discussion of possible mechanisms. *Nanoscale*. **2015**, *7* (6), 2154-2198.

(10) Dekkers, S.; Williams, T. D.; Zhang, J. K.; Zhou, J. R.; Vandebriel, R. J.; De la Fonteyne, L. J. J.; Gremmer, E. R.; He, S.; Guggenheim, E. J.; Lynch, I.; Cassee, F. R.; De Jong, W. H.;Viant, M. R. Multi-omics approaches confirm metal ions mediate the main toxicological pathways of metal-bearing nanoparticles in lung epithelial A549 cells. *Environ. Sci-Nano*. **2018**, *5* (6), 1506-1517.

(11) McCracken, C.; Dutta, P. K.;Waldman, W. J. Critical assessment of toxicological effects of ingested nanoparticles. *Environ. Sci-Nano*. **2016**, *3* (2), 256-282.

(12) Bouwmeester, H.; van der Zande, M.;Jepson, M. A. Effects of food-borne nanomaterials on gastrointestinal tissues and microbiota. *WIREs Nanomed. Nanobi.* **2018**, *10* (1), e1481.

(13) Carlander, D.; Karlsson, H.; Laloy, J.; Sabella, S.; Zande, M. v. d.; Rey-Castro, C.;Tantra, R., *NANoREG Deliverable D 5.2: Report on the development of a solubility testing procedure. CC by-nc-sa/4.0/ license*, 2015; https://www.rivm.nl/en/About_RIVM/Mission_and_strategy/International_Affairs/International_Projects/Completed/NANoREG.

(14) Tantra, R.; Bolea, E.; Bouwmeester, H.; Rey-Castro, C.; David, C. A.; Dogné, J. M.; Laborda, F.; Laloy, J.; Robinson, K. N.; Undas, A. K.;Van Der Zande, M. Solubility Part 1: Overview. In *Nanomaterial Characterization: An Introduction*; Tantra, R., Ed.; Wiley: New Jersey 2016; pp. 81-116.

(15) Tantra, R.; Bouwmeester, H.; Bolea, E.; Rey-Castro, C.; David, C. A.; Dogne, J. M.; Jarman, J.; Laborda, F.; Laloy, J.; Robinson, K. N.; Undas, A. K.;van der

Zande, M. Suitability of analytical methods to measure solubility for the purpose of nanoregulation. *Nanotoxicology*. **2016**, *10* (2), 173-184.

(16) Quadros, M. E.; Pierson, R.; Tulve, N. S.; Willis, R.; Rogers, K.; Thomas, T. A.;Marr, L. C. Release of silver from nanotechnology-based consumer products for children. *Environ. Sci. Technol.* **2013**, *47* (15), 8894-8901.

(17) Galceran, J.; Companys, E.; Puy, J.; Cecilia, J.;Garces, J. L. AGNES: a new electroanalytical technique for measuring free metal ion concentration. *J. Electroanal. Chem.* **2004**, *566* (1), 95-109.

(18) Companys, E.; Galceran, J.; Pinheiro, J. P.; Puy, J.;Salaun, P. A review on electrochemical methods for trace metal speciation in environmental media. *Curr. Opin. Electrochem.* **2017**, *3* (1), 144-162.

(19) Tehrani, M. H.; Companys, E.; Dago, A.; Puy, J.;Galceran, J. Free indium concentration determined with AGNES. *Sci. Total Environ.* **2018**, *612* 269-275.

(20) Galceran, J.; Huidobro, C.; Companys, E.;Alberti, G. AGNES: A technique for determining the concentration of free metal ions. The case of Zn(II) in coastal Mediterranean seawater. *Talanta*. **2007**, *71* (4), 1795-1803.

(21) Companys, E.; Puy, J.;Galceran, J. Humic acid complexation to Zn and Cd determined with the new electroanalytical technique AGNES. *Environ. Chem.* **2007**, *4* (5), 347-354.

(22) Companys, E.; Naval-Sanchez, M.; Martinez-Micaelo, N.; Puy, J.;Galceran, J. Measurement of free zinc concentration in wine with AGNES. *J. Agr. Food Chem.* **2008**, *56* (18), 8296-8302.

(23) Zavarise, F.; Companys, E.; Galceran, J.; Alberti, G.;Profumo, A. Application of the new electroanalytical technique AGNES for the determination of free Zn concentration in river water. *Anal. Bioanal. Chem.* **2010**, *397* (1), 389-394.

(24) Pernet-Coudrier, B.; Companys, E.; Galceran, J.; Morey, M.; Mouchel, J. M.; Puy, J.; Ruiz, N.;Varrault, G. Pb-binding to various dissolved organic matter in urban aquatic systems: Key role of the most hydrophilic fraction. *Geochim. Cosmochim. Ac.* **2011**, *75* (14), 4005-4019.

(25) Chito, D.; Galceran, J.; Companys, E.;Puy, J. Determination of the Complexing Capacity of Wine for Zn Using the Absence of Gradients and Nernstian Equilibrium Stripping Technique. *J. Agr. Food Chem.* **2013**, *61* (5), 1051-1059.

(26) Parat, C.; Authier, L.; Castetbon, A.; Aguilar, D.; Companys, E.; Puy, J.; Galceran, J.;Potin-Gautier, M. Free Zn^{2+} determination in natural freshwaters of the Pyrenees: towards on-site measurements with AGNES. *Environ. Chem.* **2015**, *12* (3), 329-337.

(27) Pearson, H. B. C.; Galceran, J.; Companys, E.; Braungardt, C.; Worsfold, P.; Puy, J.;Comber, S. Absence of Gradients and Nernstian Equilibrium Stripping (AGNES) for the determination of [Zn^{2+}] in estuarine waters. *Anal. Chim. Acta*. **2016**, *912* 32-40.

(28) Lao, M.; Companys, E.; Weng, L. P.; Puy, J.;Galceran, J. Speciation of Zn, Fe, Ca and Mg in wine with the Donnan Membrane Technique. *Food Chem.* **2018**, *239* 1143-1150.

(29) Domingos, R. F.; Huidobro, C.; Companys, E.; Galceran, J.; Puy, J.;Pinheiro, J. P. Comparison of AGNES (absence of gradients and Nernstian equilibrium stripping) and SSCP (scanned stripping chronopotentiometry) for trace metal speciation analysis. *J. Electroanal. Chem.* **2008**, *617* (2), 141-148.

(30) Rocha, L. S.; Companys, E.; Galceran, J.; Carapuca, H. M.;Pinheiro, J. P. Evaluation of thin mercury film rotating disk electrode to perform absence of gradients and Nernstian equilibrium stripping (AGNES) measurements. *Talanta*. **2010**, *80* (5), 1881-1887.

(31) Duval, J. F. L.; Farinha, J. P. S.;Pinheiro, J. P. Impact of Electrostatics on the Chemodynamics of Highly Charged Metal-Polymer Nanoparticle Complexes. *Langmuir*. **2013**, *29* (45), 13821-13835.

(32) Vale, G.; Franco, C.; Diniz, M. S.; dos Santos, M. M. C.;Domingos, R. F. Bioavailability of cadmium and biochemical responses on the freshwater bivalve Corbicula fluminea - the role of TiO_2 nanoparticles. *Ecotox. Environ. Safe.* **2014**, *109* 161-168.

(33) Vale, G.; Franco, C.; Brunnert, A. M.;dos Santos, M. M. C. Adsorption of Cadmium on Titanium Dioxide Nanoparticles in Freshwater Conditions - A Chemodynamic Study. *Electroanal.* **2015**, *27* (10), 2439-2447.

(34) David, C. A.; Galceran, J.; Rey-Castro, C.; Puy, J.; Companys, E.; Salvador, J.; Monné, J.; Wallace, R.;Vakourov, A. Dissolution Kinetics and Solubility of ZnO Nanoparticles Followed by AGNES. *J. Phys. Chem. C*. **2012**, *116* (21), 11758-11767.

(35) Galceran, J.; Lao, M.; David, C.; Companys, E.; Rey-Castro, C.; Salvador, J.;Puy, J. The impact of electrodic adsorption on Zn, Cd and Pb speciation measurements with AGNES. *J. Electroanal. Chem.* **2014**, *722* 110-118.

(36) Domingos, R. F.; Franco, C.;Pinheiro, J. P. Stability of core/shell quantum dots-role of pH and small organic ligands. *Environ. Sci. Pollut. R.* **2013**, *20* (7), 4872-4880.

(37) Mu, Q.; David, C. A.; Galceran, J.; Rey-Castro, C.; Krzemiński, Ł.; Wallace, R.; Bamiduro, F.; Milne, S. J.; Hondow, N. S.; Brydson, R.; Vizcay-Barrena, G.; Routledge, M. N.; Jeuken, L. J. C.;Brown, A. P. Systematic Investigation of the Physicochemical Factors That Contribute to the Toxicity of ZnO Nanoparticles. *Chem. Res. Toxicol.* **2014**, *27* (4), 558-567.

(38) Adam, N.; Schmitt, C.; Galceran, J.; Companys, E.; Vakurov, A.; Wallace, R.; Knapen, D.;Blust, R. The chronic toxicity of ZnO nanoparticles and $ZnCl_2$ to Daphnia magna and the use of different methods to assess nanoparticle aggregation and dissolution. *Nanotoxicology*. **2014**, *8* (7), 709-717.

(39) Walczak, A. P.; Fokkink, R.; Peters, R.; Tromp, P.; Rivera, Z. E. H.; Rietjens, I. M. C. M.; Hendriksen, P. J. M.;Bouwmeester, H. Behaviour of silver nanoparticles and silver ions in an in vitro human gastrointestinal digestion model. *Nanotoxicology*. **2013**, *7* (7), 1198-1210.

(40) Jensen, K. A.; Booth, A.; Kembouche, Y.;Boraschi, D., *NANoREG Deliverable D2.06: Validated protocols for test item preparation for key in vitro and ecotoxicity studies. CC by-nc-sa/4.0/ license*, 2016; https://www.rivm.nl/en/About_RIVM/Mission_and_strategy/International_Affairs/International_Projects/Completed/NANoREG.

(41) Lao, M.; Dago, A.; Serrano, N.; Companys, E.; Puy, J.;Galceran, J. Free Zn^{2+} determination in systems with Zn-Glutathione. *J. Electroanal. Chem.* **2015**, *756* 207-211.

(42) Companys, E.; Cecilia, J.; Codina, G.; Puy, J.;Galceran, J. Determination of Zn^{2+} concentration with AGNES using different strategies to reduce the deposition time. *J. Electroanal. Chem.* **2005**, *576* (1), 21-32.

(43) Bass, M.; Li, G.;Van Stryland, E., Eds. *Handbook of optics, Vol. IV*, 3rd ed., McGraw-Hill: New York, 2010.

(44) Pourrahimi, A. M.; Liu, D.; Pallon, L. K. H.; Andersson, R. L.; Abad, A. M.; Lagaron, J. M.; Hedenqvist, M. S.; Stroem, V.; Gedde, U. W.;Olsson, R. T. Water-based synthesis and cleaning methods for high purity ZnO nanoparticles - comparing acetate, chloride, sulphate and nitrate zinc salt precursors. *Rsc. Adv.* **2014**, *4* (67), 35568-35577.

(45) Ohshima, H., *Theory of colloid and interfacial electric phenomena*, Elsevier Academic Press: Amsterdam, The Netherlands, 2006.

(46) Gustafsson, J. P., Visual MINTEQ (version 3.1), http://vminteq.lwr.kth.se.

(47) Rathnayake, S.; Unrine, J. M.; Judy, J.; Miller, A. F.; Rao, W.;Bertsch, P. M. Multitechnique Investigation of the pH Dependence of Phosphate Induced Transformations of ZnO Nanoparticles. *Environ Sci Technol*. **2014**, *48* (9), 4757-4764.

(48) Lv, J. T.; Zhang, S. Z.; Luo, L.; Han, W.; Zhang, J.; Yang, K.;Christie, P. Dissolution and Microstructural Transformation of ZnO Nanoparticles under the Influence of Phosphate. *Environ Sci Technol*. **2012**, *46* (13), 7215-7221.

(49) Herrmann, R.; Garcia-Garcia, F. J.;Reller, A. Rapid degradation of zinc oxide nanoparticles by phosphate ions. *Beilstein J. Nanotech.* **2014**, *5* 2007-2015.

(50) Xu, H. C.; Li, L.; Lv, H.; Liu, X.;Jiang, H. L. pH-dependent phosphatization of ZnO nanoparticles and its influence on subsequent lead sorption. *Environ. Pollut.* **2016**, *208* 723-731.

(51) Wagh, A. S., *Chemically bonded phosphate ceramics : twenty-first century materials with diverse applications*, Elsevier: Amsterdam, The Netherlands, 2004.

(52) Perez, L.;Nancollas, G. H. The Kinetics of Crystallization of Hopeite. *J. Cryst. Growth*. **1984**, *66* (2), 412-418.

(53) Frohlich, E.;Roblegg, E. Models for oral uptake of nanoparticles in consumer products. *Toxicology*. **2012**, *291* (1-3), 10-17.

(54) Ngamchuea, K.; Batchelor-McAuley, C.;Compton, R. G. The fate of silver nanoparticles in authentic human saliva. *Nanotoxicology*. **2018**, *12* (4), 305-311.

(55) Calatayud, M.; Xiong, C.; Du Laing, G.; Raber, G.; Francesconi, K.;van de Wiele, T. Salivary and Gut Microbiomes Play a Significant Role in in Vitro Oral Bioaccessibility, Biotransformation, and Intestinal Absorption of Arsenic from Food. *Environ Sci Technol*. **2018**, *52* (24), 14422-14435.

Tables

Table 1: Composition of the synthetic saliva used in the experiments.[39] *This recipe was used to prepare two different synthetic solutions: saliva I (containing only the inorganic components), and saliva II (containing both inorganic and organic components).*

Inorganic components (Saliva I and II)	***Organic components*** (Saliva II)
896 mg·L^{-1} KCl	200 mg·L^{-1} urea
200 mg·L^{-1} KSCN	290 mg·L^{-1} amylase [a]
1021 mg·L^{-1} $NaH_2PO_4 \cdot H_2O$	15 mg·L^{-1} uric acid
570 mg·L^{-1} Na_2SO_4	25 mg·L^{-1} mucin [b]
298 mg·L^{-1} NaCl	
1694 mg·L^{-1} $NaHCO_3$	
pH = 6.80 ± 0.10, I = 0.0586 mol·L^{-1} [c]	

[a]: α-Amylase from *Bacillus sp.* Type II-A, lyophilized powder from Sigma-Aldrich, 50-55 kDa mol. wt.

[b]: Mucin 75-95 %, for biochemistry, isolated from porcine stomach lining, from Carl Roth GmbH.

[c]: ionic strength value calculated with Visual MINTEQ

673 # Figures
674

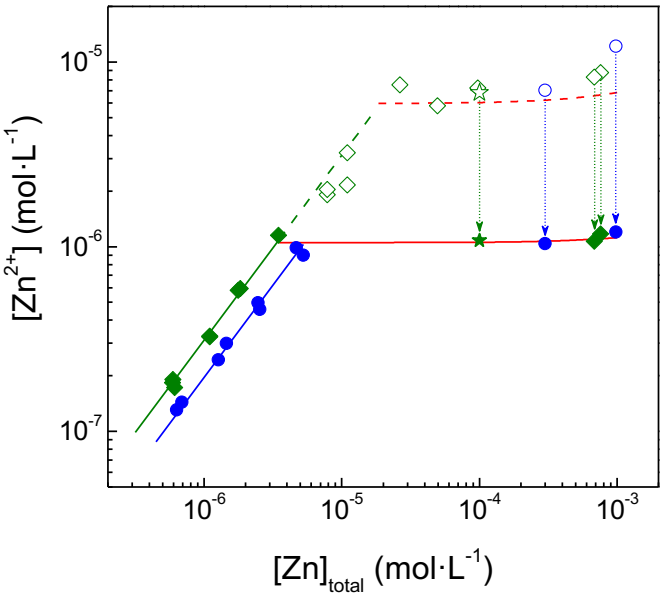

675

676 *Figure 1: Free Zn^{2+} concentrations in saliva I (green diamonds) and saliva II (blue*
677 *circles) measured by AGNES as a function of the total Zn concentration in the*
678 *dispersions, $[Zn]_{total}$. Filled markers represent equilibrium values while open markers*
679 *correspond to metastable values. Diamonds and circles: addition of ZnO NPs. Stars:*
680 *addition of dissolved Zn standard (control). The arrows connect initial (metastable) and*
681 *final (equilibrium) values within the same experiment. The red lines represent the*
682 *values of $[Zn^{2+}]$ determined by the solubility of $ZnHPO_{4(s)}$ (dashed line) and hopeite*
683 *(solid line), as calculated with Visual MINTEQ.*
684

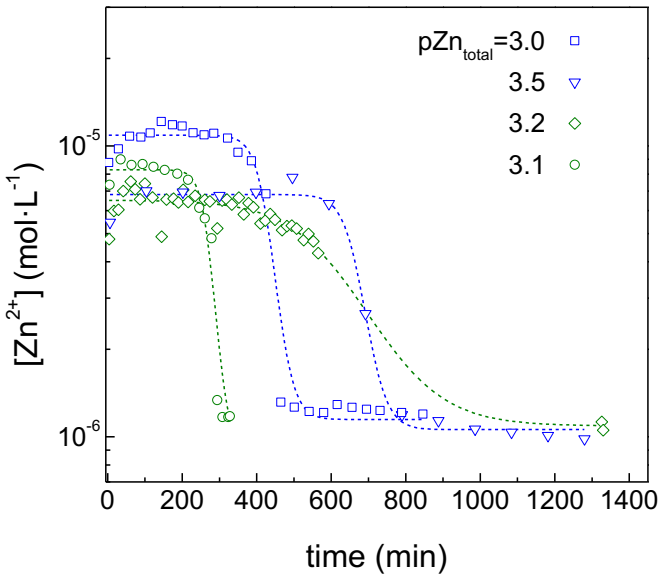

Figure 2: Representative examples of the evolution of free Zn^{2+} concentration (measured by AGNES) vs. time elapsed since the addition of ZnO NPs to saliva I (green) and saliva II (blue). The values of total Zn concentration, expressed as -log$[Zn]_{total}$ =pZn_{total} (concentrations in mol·L^{-1}), of each experiment are indicated in the legend. The dashed lines are sigmoidal fits and a guide to the eye. The variability among curves is due to small differences in the experimental values of pZn_{total} and pH.

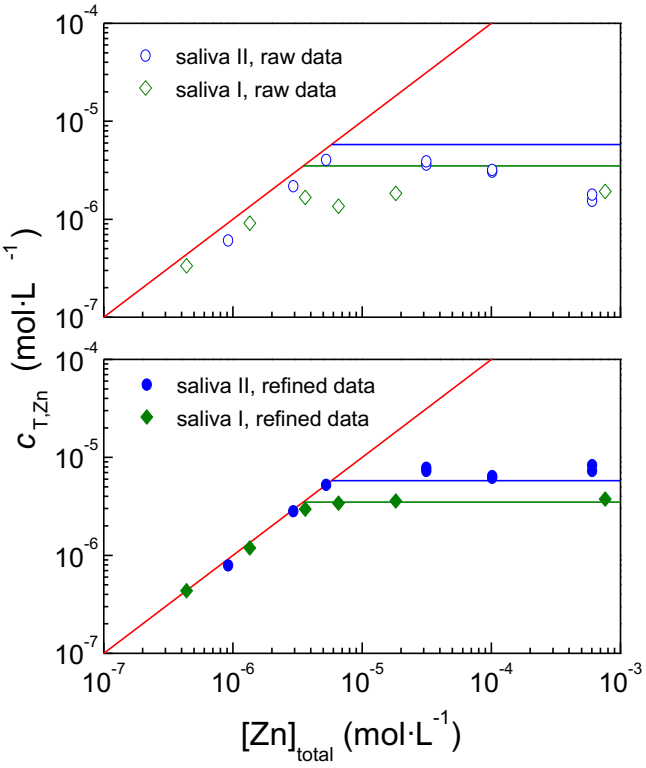

694

695 *Figure 3: Concentration of dissolved zinc species in synthetic saliva I (green diamonds)*
696 *and saliva II (blue circles) measured by UF-ICP-MS. Upper panel: raw data (open*
697 *markers). Lower panel: data corrected for loss of Zn due to adsorption on the filters,*
698 *and for pH changes during incubation using Visual MINTEQ (filled markers). The*
699 *reference pH value is 6.8. The red line represents complete dissolution. Horizontal lines*
700 *represent the effective solubilities in saliva I (green) and II (blue) according to eq. (5),*
701 *as obtained by AGNES.*
702
703